Analyst

Volume 1 | Number 1 | Jan 2013 | Pages 1–100

Analyst

www.rsc.org/analyst

Journal Name

ARTICLE

Silver nanoparticles aggregates on metal fiber for solid phase microextraction-surface enhanced Raman spectroscopy detection of polycyclic aromatic hydrocarbons

Cuicui Liu,[a] Xiaoli Zhang,[a] Limei Li,[b] Jingcheng Cui,[a] Yu-e Shi,[a] Le Wang[c] and Jinhua Zhan[,a]*

Solid phase microextraction (SPME), a solvent free technique for sample preparation, has been successfully coupled with GC，GC-MS, HPLC for environmental analysis. In this work, a method of the combing solid phase microextraction with surface enhanced Raman spectrum (SERS) was developed for detection of polycyclic aromatic hydrocarbons (PAHs). Sliver nanoparticles aggregates were deposited on the Ag-Cu fiber via layer-by-layer deposition, which were modified with propanethiol (PTH). The SERS-active SPME fiber was immersed into water directly to extract PAHs and then detected by a portable Raman spectrometer. The pronounced valence vibration of the C–C bond at 1030 cm^{-1} was chosen as an internal standard peak for its constant concentration of PTH. The (RSD) of the stability and the uniformity of the SERS-active SPME fiber are 2.97% and 5.66%, respectively. A log-log plot of the normalized SERS intensity versus fluoranthene concentration showed a liner relationship (R^2=0.95). The detection limit was $7.56×10^{-10}$ M and the recovery rate of water samples was range from 95% to 115%. The method could also be applied to detection of PAH mixtures, and each component of the mixtures could be distinguished by Raman characteristic peaks. The SERS-active SPME fiber could be further confirmed by GC-MS.

Introduction

Polycyclic aromatic hydrocarbons (PAHs), a kind of typical persistent organic pollutant,[1] have attracted worldwide attention for their strong carcinogenic, mutagenic and biological accumulating properties.[2-4] The toxicity of PAHs can be enlarged more times by ingesting food and drinking water. Due to the low content of PAHs in environmental matrix, the enrichment concentration of PAHs is generally required before their detection. Sample pretreatment technologies, such as liquid-liquid extraction,[2, 5] Soxhlet extraction[6] and chromatography[7] have been developed for enrichment of PAHs. The extraction and separation principles of these pretreatment methods are usually based on the different partition coefficient of analyte between the stationary and mobile phases.

Solid phase microextraction (SPME), a solvent-free technique, could separate and preconcentrate target analytes from complex sample matrices simultaneously and efficiently.[8, 9] SPME was commonly used to partition and preconcentrate analytes from gas or liquid phase into the coating and desorption of concentrated analytes. It has been successfully applied to environmental analysis,[10-12] food analysis,[13, 14] biological analysis,[15-17] and pharmaceutical analysis,[18, 19] etc. The pretreated sample matrix by SPME could be further identified and quantified by gas chromatography (GC),[17] gas chromatography-mass spectrometer (GC-MS),[14, 15] high performance liquid chromatography (HPLC)[20, 21] and capillary electrophoresis (CE).[22] Running solvent was generally needed during the desorption of the analytes in HPLC and capillary electrophoresis detection.[20, 21] On the other hand, infrared spectroscopy has also been developed to identify volatile organic compounds preconcentrated by solid phase microextraction.[23]

Raman spectroscopy, a kind of molecular vibration spectrum, can provide structural characteristics of the molecule.[24] Raman spectroscopy has also been developed to detect analytes pretreated by SPME.[25, 26] Surface enhanced Raman spectroscopy (SERS) can greatly amplify the Raman signal of the measured molecular, even the detailed vibration modes of molecules adsorbed on noble metal surface can be offered, which greatly extended the application of Raman spectroscopy.[27-32] Electromagnetic enhancing and chemical enhancing have made significant contributions to the SERS

a. National Engineering Research Center for Colloidal Materials and Key Laboratory for Colloid and Interface Chemistry of Ministry of Education, Department of Chemistry, Shandong University, Jinan 250100, China.
b. Department of Physics, Xiamen University, Xiamen Fujian, 361005, P. R. China
c. Center of Technology, Jinan Entry-Exit Inspection and Quarantine Bureau, Jinan 250014, China
† Footnotes relating to the title and/or authors should appear here.
Electronic Supplementary Information (ESI) available: [details of any supplementary information available should be included here]. See DOI: 10.1039/x0xx00000x

effect.[33-36] Electromagnetic enhancing is caused by localized surface plasmon resonances of compounds adsorbed on roughened metal surfaces, which can multiply the scattering intensity by 10^4-10^6. Chemical enhancement is considered as the bonding interactions of the adsorbate-substrate, which can enhance scattering cross section to the order 10^2.[36, 37] Various substrates are composed of shaped particles,[38-45] vapor-deposited films,[46] functionalized metal nanostructures,[47, 48] colloidal suspensions[49] and bimetallic nanostructures,[50, 51] which can offer good enhancement and has been used for sample identification such as environmental pollutants,[35, 52, 53] explosives,[44] food additives,[54] DNA bases,[55] therapeutic agents,[56] drug of abuse,[57] cells and spores,[48, 58] pesticide residues.[59]

In this paper, we developed a SERS-active SPME fiber combining the advantages of SPME and SERS. The Ag-Cu fiber was coated with silver nanoparticles by galvanic displacement reaction with $SnCl_2$ as the "sensitizer". After propanethiol modified on the surface of silver nanoparticles, the fiber was SERS active for PAHs. The SERS-active SPME fiber was immersed into water directly to extract PAHs and then detected by a portable Raman spectrometer. The SERS-active SPME fiber could be further confirmed by GC-MS. The SPME-SERS reduces the sample pretreatment and shortens the total analysis time, providing an in-situ detection technique.

Experiment

Chemicals

Silver nitrate ($AgNO_3$) and PVP-K30 were purchased from Sinopharm Chemical Reagent Co., Limited. Silver-copper alloy fiber (ID, 0.35 cm, Ag:Cu=1:1) was purchased from ZhongNuo Advanced Material (Beijing) Technology Co., Limited. Propanethiol ($CH_3(CH_2)_2SH$) (PTH), Tin dichloride ($SnCl_2 \cdot 2H_2O$) and benzo(b)fluoranthene (4.39 μg/mL) in methanol were obtained from Aladdin Chemistry Co., Ltd. Fluoranthene (›98%, GC) and pyrene (98%) were purchased from Tokyo Chemical Industry. Fluoranthene was dissolved in ethanol to get a solution at 10^{-3} mol·L^{-1}. Fluoranthene solutions of low concentration were obtained by diluting the high-concentration solution with ultrapure water. Ultra-pure water (18.25 MΩ·cm^{-1}) was used throughout the experiment.

Characterization techniques and SERS detection

The morphology of the SERS-active fiber was characterized by scanning electron microscope (SEM) (JSM-6700F). X-ray photoelectron spectroscopy (XPS) measurements of the PTH modified silver nanoparticles fiber was performed with X-Ray Photoelectron Spectroscopy (ESCALAB 250, ThermoFisher SCIENTIFIC). All the Raman measurements were carried out by an Ocean Optics QE65000 spectrometer. The excitation wavelength was 785 nm, the input laser power was 440 mw, and the integration time was 1 s. An Agilent GC system (7890A, Palo Alto, USA) coupled with mass spectrometer (5973N, Agilent, USA) was used for all the experiments. GC separation was performed using a fused silica AB-5MS capillary column with a length of 30 m × 0.25 mm and a film thickness of 0.50 μm (J&W Scientific, USA). The oven temperature was held at 100°C for 2.0 min. The succeeding oven temperatures were programmed to increase as follows: at 10°C min^{-1}

to 280°C and held for 12.0 min. Helium (99.999%) was used as the carrier gas at a flow rate of 1 mL/min. The mass spectrometer was operated in electron impact ionization (EI) mode with an ionizing energy of 70.0 eV. The analytes were thermal desorption for 2 min.

Preparation of the SERS-active SPME fiber

The silver-copper alloy fiber was washed separately with acetone, ethanol and ultra-pure water under ultrasonic irradiation for 10 min, and then immersed in 0.1 M HNO_3 aqueous solution for 1 min to remove the surface oxide layer. The treated silver-copper alloy fiber was washed with ultra-pure water and dried for further use. The silver-copper alloy fiber was first immersed into the solution of $SnCl_2$ (0.02 M) and HCl (0.02 M) for 1 min to absorb Sn^{2+} on the surface, then dried at room temperature. Next, silver-copper alloy fiber was immersed into the solution of $AgNO_3$ (0.01 M) and PVP for 1 min to deposit silver nanoparticles on the surface.[60] The weight ratio of $AgNO_3$: PVP was kept at 2:1. Repeated the above two steps in a cyclic fashion. Finally, the fiber was immersed into the Sn^{2+} solution once again and washed with ultra-pure water. Typically, sixteen cycles were used for the following experiments. The fiber was immersed into 1 mM propanethiol solution for 12 h at room temperature. The SERS-active SPME fiber was immersed into the test solution (25 mL). The samples were stirred for 180 min at a constant speed (500 rpm). SPME analysis was performed at 25℃.

Results and discussion

Fabrication and Characterization of the SPME fiber

Scheme 1 depicted the process of the SERS-active SPME fiber detection. The silver nanoparticles aggregates on silver-copper fiber were prepared via galvanic displacement reaction with $SnCl_2$ as the "sensitizer" in the previous report.[60] Propanethiol was selected as modifier on the surface of silver nanoparticles, which protect silver nanoparticles from oxidation (see Figure S1 and Figure S2), preconcentrate PAHs and act as an internal standard in quantitative analysis. The SPME fiber was selected as the SERS-active substrate for their good SERS performance of silver nanoparticles. The SERS-active SPME fiber was put on the platform and irradiated by the laser, and then the Raman spectra were obtained. The SERS-active SPME fiber could be further confirmed by GC-MS.
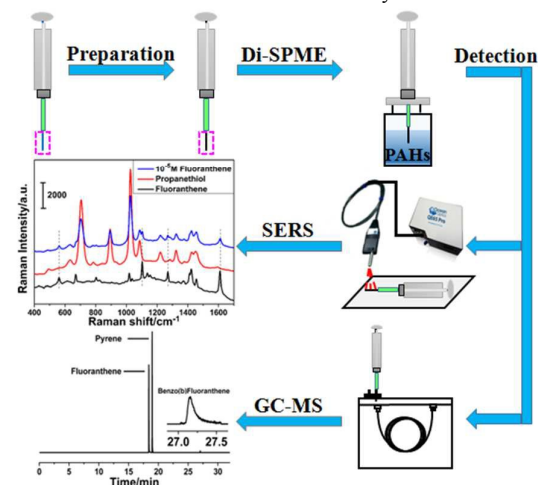
Scheme. 1 Illustration of silver nanoparticles loaded onto silver-copper fiber used for SPME-SERS detection.

The morphology of the commercial Ag-Cu fiber and the prepared SERS-active SPME fiber were characterized by scanning electron microscope, as illustrated by Figure S3 and Figure S4. Compared with commercial Ag-Cu fiber, the morphology of AgNPs/Ag-Cu fiber was covered with dense silver nanoparticles aggregates (Figure S4A). The morphology of AgNPs/Ag-Cu fiber had no obvious change with increase the number of circulation (Figure S4B). The modification with PTH had little difference on the morphology of the AgNPs/Ag-Cu fiber (Figure S4C). The thickness of the silver nanoparticles aggregates on the silver-copper fiber after sixteen cycles was about 6 μm, as shown by the cross-sectional SEM image in Figure S4D. The enhancement factor (EF) of the AgNPs/Ag-Cu fiber probing p-aminothiophenol, calculated to the refence,[61] is $1.59×10^5$. (see the EF calculation in ESI)

The presence of PTH could be further verified by X-ray photoelectron spectroscopy (XPS), as shown in Figure S5 and Figure S6. The full XPS spectra of the PTH modified AgNPs/Ag-Cu fiber indicated the presence of both silver and sulfur element (Figure S5A). The binding energy of the $Ag3d_{5/2}$ and $Ag3d_{3/2}$ was centered at 368.10 eV and 374.10 eV, respectively (Figure S5B). The binding energy of the S2p was centered at 162.05 eV (Figure S5C), which agreed with the previous reports.[62] Silver binding energy shifted to lower value by 0.2 eV might be attributing to the formation of Ag-S bond (Figure S5D). The Ag3d spectra analysis also suggested two distinct chemical states for Ag (Figure S6).
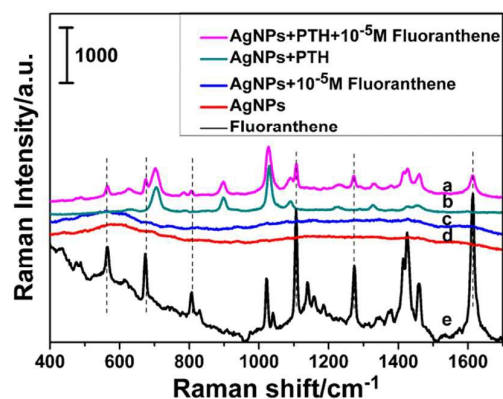
Figure 1. (a) SERS spectra of $1.00×10^{-5}$ M fluoranthene on the PTH modified AgNPs/Ag-Cu fiber. (b) SERS spectra of the PTH modified AgNPs/Ag-Cu fiber. (c) SERS spectra of $1.00×10^{-5}$ M fluoranthene on the AgNPs/Ag-Cu fiber without propanethiol. (d) Raman spectrum of AgNPs/Ag-Cu fiber. (e) Raman spectrum of fluoranthene power.

To confirm whether fluoranthene could be adsorbed onto SERS-active SPME fibers, the fibers were immersed in $1.00×10^{-5}$ M fluoranthene solution for 180 min and their SERS spectra were recorded, as shown in Figure 1. Figure 1a showed the SERS spectrum of fluoranthene onto SERS-active SPME fiber in the region from 400 to 1700 cm^{-1}. The Raman spectrum of fluoranthene was also shown for comparison in Figure 1e, which conformed with the FT-Raman spectrum of the powder sample of fluoranthene.[63] Figure 1b illustrated the SERS spectra of the functional fiber with propanethiol. The Raman spectrum of liquid propanethiol was also recorded for comparison (see Figure S7). Compared with the normal Raman spectrum of liquid propanethiol, both the number of Raman

peaks and relative intensities had some differences.[64, 65] It could be seen that the native AgNPs/Ag-Cu fiber had no SERS signals of fluoranthene, as shown in Figure 1c. A comparison between Figure 1a and Figure 1e clearly indicated that the Raman characteristic peak of fluoranthene at 1612 cm^{-1} could be seen. These results indicate propanethiol acts as the extracting agent to extract fluoranthene from the aqueous solution.

Alkanethiols, forming hydrophobic layers on the silver nanostructures, could preconcentrate multiple hydrophobic compounds.[60, 63, 66] To evaluate enhancement effect of different alkanethiol, the different alkanethiol modified AgNPs/Ag-Cu fibers were immersed into $1.00×10^{-5}$ M fluoranthene solution for 3 h and their SERS spectra were recorded. The SERS spectra of fluoranthene on the substrate with different alkanethiol are shown in Figure S8. Among these alkanethiols, PTH modified AgNPs/Ag-Cu fiber showed the best performance, suggesting that the SERS intensity is dependent on the distance of the alkanethiol from the silver nanoparticles surface.[67] The results could be further demonstrated by theoretically calculated with finite-difference time-domain (FDTD). Figure S9 showed the near-field enhancement of the silver nanoparticles at 785 nm excitation. The large electromagnetic enhancement is caused by the localized surface plasmon resonances excited on the surface of the metal, which is approximately $(E)^4$.[68] The electromagnetic enhancement factor (EF) of SERS intensity depends on the distance of CH_3- from the surface of silver nanoparticles (d) and the average radius of the silver nanoparticles (r), which was calculation by the formula $EF=K(E)^4$.

In the formula, $K \approx (\frac{r+d}{r})^{-12}$.[69]

The length of the three alkanethiols was about 0.418 nm, 0.788 nm, 1.55 nm, respectively (see Figure S10). The results indicated electromagnetic enhancement factor of propanethiol was the strongest (see Figure S11). Hence, propanethiol have been considered as the best surface modification materials for detecting PAHs by SERS techniques.

To evaluate enhancement effect of the SERS-active SPME fiber under different cycle number, the PTH modified AgNPs/Ag-Cu fibers were immersed into $1.00×10^{-5}$ M fluoranthene solution for 180 min and their SERS spectra were recorded (Figure S12). It showed the Raman intensity underwent a gradual increase until sixteen cycles. Sixteen cycles was selected for the following experiments due to its high enhancement.

Stability, Uniformity and Reproducibility of the SERS-active SPME fiber

To obtain reliable SERS signals, the evaluation of stability and uniformity of the SERS-active SPME fiber are crucial to SERS detection. The temporal stability of the fiber probed with $1.00×10^{-5}$ M fluoranthene was evaluated. The SERS spectra of fluoranthene were recorded for 5 min under continuous laser radiation with laser powers at 440 mw, as shown in Figure 2A. It could be seen that the temporal stability of the SERS-active SPME fiber under continuous laser radiation for 5 min had no obvious change. The RSD of the intensity change of the Raman peak at 1612 cm^{-1} was 2.97%. For routine SERS analysis, the SERS-active SPME fiber should be stable for a long period of time.[70, 71] The stability was evaluated by

Analyst Accepted Manuscript

comparing the freshly prepared SERS-active SPME fiber with the fibers stored in air. After different prolonged storage, SERS spectra of 1.00×10^{-5} M fluoranthene aqueous solution were recorded, as shown in Figure S13A. Compared with the Raman spectrum of fluoranthene on the freshly fiber, the Raman shift showed little change. The RSD of the intensity change of the normalized Raman peak at 1612 cm^{-1} was 5.73%, as shown in Figure S13B. The results demonstrate the very good stability of the fiber is required for practical SERS detection.

Furthermore, the uniformity of the SERS-active SPME fiber under continuous laser irradiation is also play an important role in SERS detection. The SERS spectra of twenty points were randomly selected from the PTH modified AgNPs/Ag-Cu fiber probed with 1.00×10^{-5} M fluoranthene for the evaluation of the uniformity of the SERS-active SPME fiber (Figure S14). The relative standard deviation of the intensity of fluoranthene at 1612 cm^{-1} was 16.07%.
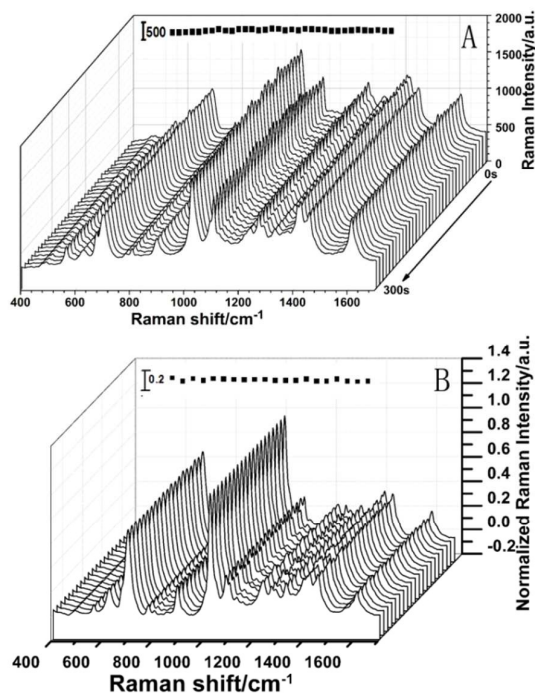
Figure 2. (A) SERS spectra of the SERS-active SPME fiber probed with 1.00×10^{-5} M fluoranthene under continuous laser radiation. (B) The uniformity of the SERS-active SPME fiber probed with 1.00×10^{-5} M fluoranthene (the SERS spectra were normalized using the Raman peak of the PTH at 1030 cm^{-1} as the reference). The inset image shows the changes of the Raman peak of fluoranthene at 1612 cm^{-1}.

The SERS intensity could be proved by the following formula:

$$I_{SERS} \propto N I_L |A(\nu_L)|^2 |A(\nu_S)|^2 \sigma_{ads}^R \qquad (1)^{72}$$

In the format, I_{SERS} is the SERS signal, N is the number of the adsorption molecules involved in the SERS process, I_L is the excitation intensity, $A(\nu_L)$ and $A(\nu_S)$ are excitation and scattered field enhancement factors, σ_{ads}^R is the increased Raman cross section of the adsorbed molecule.

Assuming a, b, c … are random spots on the PTH modified AgNPs/Ag-Cu fiber,

$$N_a \neq N_b \neq N_c \neq N_\dots \qquad (2)$$
$$|A(\nu_L)|_a^2 |A(\nu_S)|_a^2 \neq |A(\nu_L)|_b^2 |A(\nu_S)|_b^2 \neq |A(\nu_L)|_c^2 |A(\nu_S)|_c^2 \neq |A(\nu_L)|_\dots^2 |A(\nu_S)|_\dots^2 \qquad (3)$$

The SERS intensity fluctuated owing to the fact that the adsorbed molecular number, the fluctuation in the Raman spectrometer and the variation of the excitation and the scattered field enhancement factor may vary from spot to spot.

$$I_{SERS,\ a} \neq I_{SERS,\ b} \neq I_{SERS,\ c} \neq I_{SERS,\ \dots} \qquad (4)$$

Besides PAHs, the SERS intensity of PTH on SPME fiber may also fluctuate. The RSD of the pronounced Raman peak of PTH at 1030 cm^{-1} was 15.01% (Figure S8). At a particular spot on the PTH modified AgNPs/Ag-Cu fiber, I_L, $A(\nu_L)$ and $A(\nu_S)$ were the same for PTH and fluoranthene. For a specific molecule, the σ^R is a constant, hence

$$I_{Normalized} = \frac{I_{SERS,\ Fluor}}{I_{SERS,\ PTH}} = k \frac{N_{Fluor}}{N_{PTH}} \qquad (5)$$

On the other hand, the adsorption in solution could generally be explained by Freundlich isotherm equation.[73]

$$\frac{N_{Fluor}}{N_{PTH}} = k_1 c^{\frac{1}{n}} \qquad (6)$$

c is the concentration of the fluoranthene, k_1 and n are constant for a certain system at a certain temperature. In a certain solution, the ratio of fluoranthene to PTH for different spots may be equal.

$$\frac{N_{Fluor,\ a}}{N_{PTH,\ a}} = \frac{N_{Fluor,\ b}}{N_{PTH,\ b}} = \frac{N_{Fluor,\ c}}{N_{PTH,\ c}} = \frac{N_{Fluor,\ \dots}}{N_{PTH,\ \dots}} \qquad (7)$$

The possible structures of S-C-C chain were trans and gauche conformation. N-alkanethiols on the solid surface mostly exist in trans conformation.[74] The vibrational modes of Raman peak of PTH at 1030 cm^{-1}, 1090 cm^{-1} were trans and gauche conformation, respectively. If the Raman peak of PTH at 1030 cm^{-1} was selected as an internal standard peak, the RSD of the intensity change of the Raman peak at 1612 cm^{-1} was 5.66%, as shown in Figure 2B. If the Raman peak of PTH at 1090 cm^{-1} was selected as an internal standard peak, the RSD of the intensity change of the Raman peak at 1612 cm^{-1} was 7.51% (see Table S1). Normalization improved the uniformity for reducing the variation of adsorbed molecular number and fluctuation of the excitation and scattered field.

Besides, the reproducibility of the SERS signal intensity is very important for routine SERS analysis. The SERS-active SPME fibers were immersed into 1.00×10^{-8} M fluoranthene solution for 3 hour to reach equilibrium and their SERS spectra were recorded (Figure S15). The relative standard deviation of the normalized Raman intensity of fluoranthene at 1612 cm^{-1} was 9.09%. This result confirmed that the SERS-active SPME fibers had good reproducibility.

SPME optimizations

To achieve higher SERS intensity, several factors including the curve equilibrium, agitation and extraction temperature are needed to be optimized. A standard working solution of 1.00×10^{-5} M (fluoranthene) was used for the optimization experiments. Extraction efficiency can be improved under agitation. Agitation can improve the rate of mass transfer of analytes between the solution and SPME fiber. Figure 3A showed the Raman intensity was higher under agitation.

The optimization of the extraction temperature was evaluated.

Extraction temperature affects equilibrium time, the process of SPME adsorption is generally exothermic. According to Figure 3B, to obtain higher extraction efficiency, the optimal extraction temperature was 25℃.
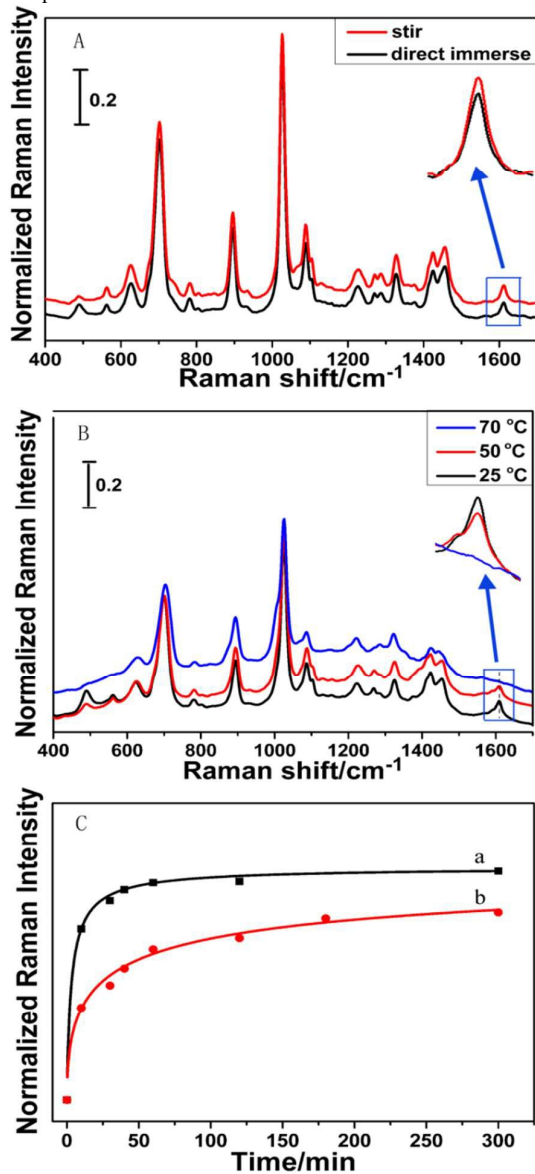
Figure 3. (A) Effect of agitation profile for the detection of fluoranthene. (B) Effect of temperature profile for the detector responses of fluoranthene. (C) Kinetic curve of (a) 1.00×10^{-7} M, (b) 1.00×10^{-8} M fluoranthene adsorption onto the SERS-active SPME fiber.

Extraction time has an impact on extraction efficiency. Extraction efficiency increases with extraction time increasing before reach adsorption equilibrium. The SERS-active SPME fibers were immersed into fluoranthene solution for 5 h, the spectra recorded at regular intervals. Figure 3C showed the kinetics of fluoranthene adsorption. For the solution with 1.00×10^{-7} M and 1.00×10^{-8} M initial fluoranthene concentration, the saturated adsorption time was 60 and 180 min, respectively.

The lower concentration of the sample, the longer time to reach adsorption equilibrium is required. To make sure the adsorption of SPME fiber reach equilibrium，a relative long time of 180 min was selected for fluoranthene extraction and detection.

SPME-SERS detection

To obtain reliable quantitative information about fluoranthene, the fibers were inserted into fluoranthene solution with various concentrations ranging from 1.00×10^{-5} M to 1.00×10^{-8} M. The SERS spectra of fluoranthene were recorded. Figure 4 showed the normalized Raman intensity of fluoranthene at 1612 cm^{-1} increased with the concentrations of fluoranthene increasing.
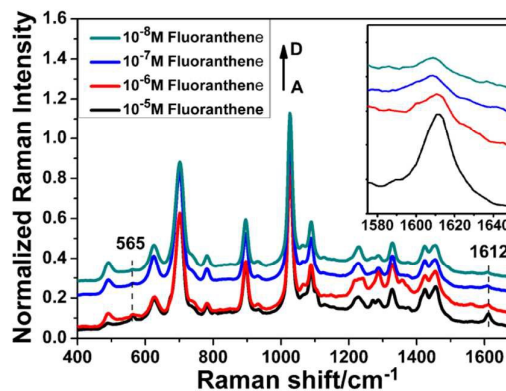
Figure 4. SERS spectra of fluoranthene on the SERS-active SPME fiber with concentrations of (A) 1.00×10^{-5} M, (B) 1.00×10^{-6} M, (C) 1.00×10^{-7} M, (D) 1.00×10^{-8} M.

The calibration curve for fluoranthene at 1612 cm^{-1} was plotted on the basis of internal standard method, as shown in Figure 5A. Figure 5A showed the normalized Raman intensity at 1612 cm^{-1} became saturated at higher concentrations for the saturation of the enhanced actives sites. The log-log plot of the normalized Raman intensity of fluoranthene at 1612 cm^{-1} versus its concentration showed a good linear relationship, as shown in Figure 5B. The liner equation was y=-1.54622+0.20912x (x is logarithm of the fluoranthene concentration, y is logarithm of the normalized SERS intensity of Raman peak at 1612 cm^{-1}, and the correlation coefficient (R^2) was 0.95). The detection limit of this method was about 7.56×10^{-10} M (see Table S2). The relationship between SERS intensity and the adsorption molecules number were obtained from the formula (5) and (6):

$$I_{Normalized} = k_2 c^{\frac{1}{n}} \qquad (8)$$

$$\log I_{Normalized} = K + \frac{1}{n}\log c \qquad (9)$$

From equation (9), the good linear relationship of the log-log plot is reasonable. The recovery rate for different concentrations of water samples ranges from 95 to 115%. The relative standard deviation (RSD) ranges from 3.85 to 6.98%, which is an acceptable RSD for SERS detection. The results indicated the SERS-active SPME fiber could be used as an exciting perspective for SPME-SERS quantitative and quantitative analysis of real samples.

COMMUNICATION
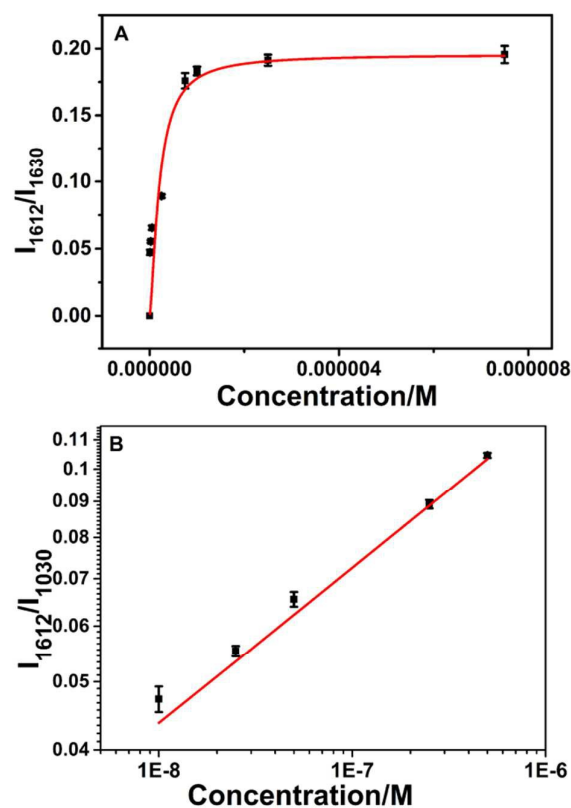
Figure 5. (A) Calibration curve. (B) log-log plot of fluoranthene based on the SERS-active SPME fibers.

To further evaluate the ability of SERS-active SPME to detect real sample, the fiber was immersed into the mixtures of PAHs. The chemical structures of the three kind of PAHs used in this work are illustrated in Figure S16. The solution was diluted with Black Tiger Spring water. Figure 6 showed the SERS
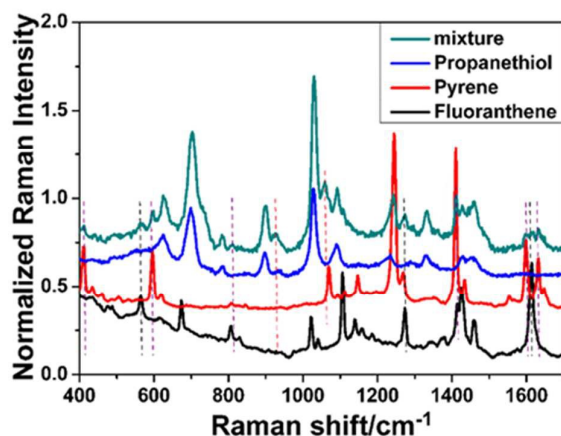
Figure 6. The SERS spectra of the PAHs mixture (1.00×10^{-5} M fluoranthene, 1.00×10^{-5} M pyrene and 1.00×10^{-7} M benzo(b)fluoranthene

spectra of the mixture. The analytes contain fluoranthene (1.00×10^{-5} M), pyrene (1.00×10^{-5} M), benzo(b)fluoranthene

(1.00×10^{-7} M). The Raman peaks of fluoranthene solution at 565 cm^{-1}, 1104 cm^{-1}, 1612 cm^{-1} were agreed with the power of fluoranthene. The Raman peaks of pyrene solution at 408 cm^{-1}, 597 cm^{-1}, 1411 cm^{-1}, 1599 cm^{-1}, 1630 cm^{-1} were also agreed with the power of pyrene. The Raman characteristic peak of benzo(b)fluoranthene solution appeared at 1603 cm^{-1}, which matched with benzo(b)fluoranthene (1.00×10^{-7} M) (see Figure S17). The results indicate all PAHs have been extracted and detected.
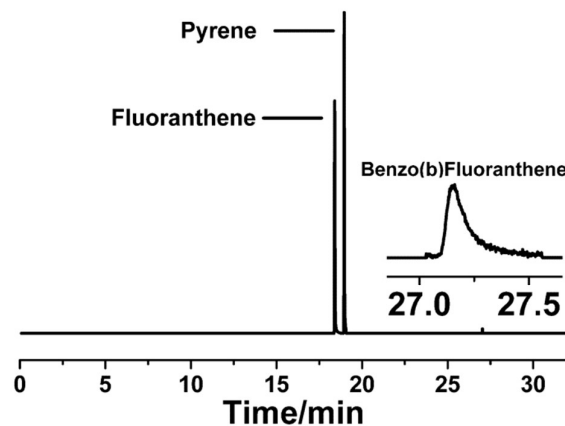
Figure 7. Extracted ion chromatograms of PAHs obtained by GC-MS**.**

The three PAH compounds on the SERS-active SPME fiber could be further confirmed by GC-MS. The fiber was immersed into the sample of PAHs mixtures containing fluoranthene (1.00×10^{-5} M), pyrene (1.00×10^{-5} M) and benzo(b)fluoranthene (1.00×10^{-7} M) for 3h, and then the fiber was put into the GC injector for desorption. As shown in Figure 7, chromatographic peak of three PAH compounds were clearly separated.

Conclusions

In this work, the SERS-active SPME fibers were fabricated to extract and detect PAHs by a portable Raman spectrometer. The fibers were prepared via galvanic displacement reaction with SnCl$_2$ as the "sensitizer". Propanethiol was selected to modify the silver nanoparticles, which played multiple roles in this work: protect Ag nanoparticles, preconcentrate PAHs close to the surface of the fibers through hydrophobic layers, and serving as an internal standard in quantitative analysis. The good uniformity and high temporal stability of the fibers indicate its potential for routine analysis. The SPME-SERS method can be used for the quantitative analysis of fluoranthene in the concentration range of 1.00×10^{-6} M to 1.00×10^{-8} M and with the detection limit of 7.56×10^{-10} M. The fiber not only can be detected and distinguished by a portable Raman spectrometer, but also can be further confirmed by GC-MS. The SERS-active SPME fibers combining of the advantages of both SPME and SERS may be extended to more widespread fields including on-site and omission detection.

Acknowledgements

Supporting information

The SI includes eighteen figures and two tables. This material is available free of charge via the Internet at http://pubs.acs.org.

Notes and references

National Engineering Research Center for Colloidal Materials and Key Laboratory for Colloid & Interface Chemistry of Education Ministry, Department of Chemistry, Shandong University, Jinan Shandong, 250100, P. R. China. E-mail: jhzhan@sdu.edu.cn

1. F. Wania, D. Mackay, *Environ. Sci. Technol.* **1996**, 30, 390A-396A.

2. Z. Li, L. C. Romanoff, D. A. Trinidad, N. Hussain, R. S. Jones, E. N. Porter, D. G. Patterson Jr, A. Sjődin, *Anal. Chem.* **2006**, 78, 5744-5751.

3. I. S. Kozin, C. Gooijer, N. H. Velthorst, *Anal. Chem.* **1995**, 67, 1623-1626.

4. A. Motelay-Massei, T. Harner, M. Shoeib, M. Diamond, G. Stern, B. Rosenberg, *Environ. Sci. Technol.* **2005**, 39, 5763-5773.

5. P. Mary, V. Studer, P. Tabeling, *Anal. Chem.* **2008**, 80, 2680-2687.

6. G. Reimer, A. Suarez, *J. Chromatogr. A.* **1995**, 699, 253-263.

7. F. L. Dorman, J. J. Whiting, J. W. Cochran, J. Gardea-Torresdey, *Anal. Chem.* **2010**, 82, 4775-4785.

8. C. L. Arthur, J. Pawliszyn, *Anal. Chem.* **1990**, 62, 2145-2148.

9. Z. Y. Zhang, M. J. Yang, J. Pawliszyn, *Anal. Chem.* **1994**, 66, 844A-853A.

10. E. Boyacı, J. Pawliszyn, *Anal. Chem.* **2014**, 86, 8916-8921.

11. J. Q. Xu, J. P. Luo, J. W. Ruan, F. Zhu, T. G. Luan, H. Liu, R. F. Jiang, G. F. Ouyang, *Environ. Sci. Technol.* **2014**, 48, 8012-8020.

12. C. J. Koester, S. L. Simonich, B. K. Esser, *Anal. Chem.* **2003**, 75, 2813-2829.

13. D. Kupryianchyk, M. I. Rakowska, I. Roessink, E. P. Reichman, J. T. C. Grotenhuis, A. A. Koelmans, *Environ. Sci. Technol.* **2013**, 47, 4563-4571.

14. O. Pinho, I. M. P. L. V. O. Ferreira, M. A. Ferreira, *Anal. Chem.* **2002**, *74*, 5199-5204.

15. C. Bancon-Montigny, P. Maxwell, L. Yang, Z. Mester, R. E. Sturgeon, *Anal. Chem.* **2002**, 74, 5606-5613.

16. G. F. Ouyang, K. D. Oakes, L. Bragg, S. Wang, H. Liu, S. F. Cui, M. R. Servos, D. G. Dixon, J. Pawliszyn, *Environ. Sci. Technol.* **2011**, 45, 7792-7798.

17. X. M. Yu, H. D. Yuan, T. Górecki, J. Pawliszyn, *Anal. Chem.* **1999**, 71, 2998-3002.

18. J. L. P. Pavón, M. d. N. Sánchez, C. G. Pinto, M. E. F. Laespada, B. M. Cordero, *Anal. Chem.* **2006**, 78, 4901-4908.

19. X. Zhang, K. D. Oakes, D. Luong, C. D. Metcalfe, J. Pawliszyn, M. R. Servos, *Anal. Chem.* **2011**, 83, 2371-2377.

20. Y. L. Hu, C. S. Song, G. K. Li, *J. Chromatogr. A.* **2012**, 1263, 21-27.

21. W. M. Mullett, K. Levsen, J. Borlak, J. C. Wu, J. Pawliszyn, *Anal. Chem.* **2002**, 74, 1695-1701.

22. S. Li, S. G. Weber, *Anal. Chem.* **1997**, 69, 1217-1222.

23. D. L. Heglund, D. C. Tilotta, *Environ. Sci. Technol.* **1996**, 30, 1212-1219.

24. D. A. Long, *Raman Spectroscopy*, **1977.**

25. J. A. Koziel, M. Odziemkowski, J. Pawliszyn, *Anal. Chem.* **2001**, 73, 47-54.

26. I. C. Nwaneshiudu, C. A. Nwaneshiudu, D. T. Schwartz, *Appl. Spectrosc.* **2014**, 68, 1254-1259.

27. D. L. Jeanmaire, R. P. V. Duyne, *J. Electroanal. Chem.* **1977**, 84, 1-20.

28. J. C. Tsang, J. R. Kirtley, J. A. Bradley, *Phys. Rev. Lett.* **1979**, 43, 772-775.

29. X. Y. Zhang, M. A. Young, O. Lyandres, R. P. Van Duyne, *J. Am. Chem. Soc.* **2005**, 127, 4484-4489.

30. J. Kneipp, X. T. Li, M. Sherwood, U. Panne, H. Kneipp, M. I. Stockman, K. Kneipp, *Anal. Chem.* **2008**, 80, 4247-4251.

31. C. J. L. Constantino, T. Lemma, P. A. Antunes, R. Aroca, *Anal. Chem.* **2001**, 73, 3674-3678.

32. I. López-Tocón, J. C. Otero, J. F. Arenas, J. V. Garcia-Ramos, S. Sanchez-Cortes, *Anal. Chem.* **2011**, 83, 2518-2525.

33. S. Huh, J. Park, Y. S. Kim, K. S. Kim, B. H. Hong, J. M. Nam, *ACS Nano* **2011**, 5, 9799-9806.

34. P. Zhang, Y. Y. Guo, *J. Am. Chem. Soc.* **2009**, 131, 3808-3809.

35. L. Guerrini, J. V. Garcia-Ramos, C. Domingo, S. Sanchez-Cortes, *Anal. Chem.* **2009**, 81, 1418-1425.

36. P. Kambhampati, C. M. Child, M. C. Foster, A. Campion, *J. Chem. Phys.* **1998**, 108, 5013-5026.

37. A. Campion, J. E. IvaneckyⅢ, C. M. Child, M. Foster, *J. Am. Chem. Soc.* **1995**, 117, 11807-11808.

38. M. J. Mulvihill, X. Y. Ling, J. Henzie, P. D. Yang, *J. Am. Chem. Soc.* **2010**, 132, 268-274.

39. A. Gutés, C. Carraro, R. Maboudian, *J. Am. Chem. Soc.* **2010**, 132, 1476-1477.

40. M. S. Wang, C. B. Gao, Q. P. Lu, J. Z. Zhang, C. Tang, S. Zorba, Y. D. Yin, *J. Am. Chem. Soc.* **2013**, 135, 15302-15305.

41. S. Shanmukh, L. Jones, J. Driskell, Y. P. Zhao, R. Dluhy, R. A. Tripp, *Nano Lett.* **2006**, 6, 2630-2636.

42. A. Tao, F. Kim, C. Hess, J. Goldberger, R. R. He, Y. G. Sun, Y. N. Xia, P. D. Yang, *Nano Lett.* **2003**, 3, 1229-1233.

43. C. H. Zhu, G. W. Meng, Q. Huang, Z. Zhang, Q. L. Xu, G. Q. Liu, Z. L. Huang, Z. Q. Chu, *Chem. Commun.* **2011**, 47, 2709-2711.

44. S. S. R. Dasary, A. K. Singh, D. Senapati, H. T. Yu, P. C. Ray, *J. Am. Chem. Soc.* **2009**, 131, 13806-13812.

45. M. Rycenga, X. H. Xia, C. H. Moran, F. Zhou, D. Qin, Z. Y. Li, Y. N. Xia, *Angew. Chem.* **2011**, 123, 5587-5591.

46. D. J. Semin, K. L. Rowlen, *Anal. Chem.* **1994**, 66, 4324-4331.

47. L. Guerrini, J. V. Garcia-Ramos, C. Domingo, S. Sanchez-Cortes, *Anal. Chem.* **2009**, 81, 953-960.

48. S. F. Zong, Z. Y. Wang, J. Yang, Y. P. Cui, *Anal. Chem.* **2011**, 83, 4178-4183.

49. R. G. Freemen, K. C. Grabar, K. J. Allison, R. M. Bright, J. A. Davis, A. P. Guthrie, M. B. Hommer, M. A. Jackson, P. C. Smith,; D. G. Walter, M. J. Natan, *Science* **1995**, 267, 1629-1632.

50. C. B. Gao, Y. X. Hu, M. S. Wang, M. F. Chi, Y. D. Yin, *J. Am. Chem. Soc.* **2014**, 136, 7474-7479.

51. J. J. Qiu, Y. C. Wu, Y. L. Wang, M. H. Engelhard, L. McElwee-White, W. D. Wei, *J. Am. Chem. Soc.* **2013**, 135, 38-41.

52. D. Li, D. W. Li, J. S. Fossey, Y. T. Long, *Anal. Chem.* **2010**, 82, 9299-9305.

53. L. L. Qu, T. T. Li, D. W. Li, J. Q. Xue, J. S. Fossey, Y. T. Long, *Analyst* **2013**, 138, 1523-1528

54. M. Lin, L. He, J. Awika, L. Yang, D. R. Ledoux, H. Li, A. Mustapha, *J. Food, Sci.* **2008**, 73, T129-T134.

55. K. Kneipp, H. Kneipp, V. B. Kartha, R. Manoharan, G. Deinum, I. Itzkan, R. R. Dasari, M. S. Feld, *Phys. Rev. E* **1998**, 57, R6281-R6284.

56. R. J. Stokes, E. McBride, C. G. Wilson, J. M. Girkin, W. E. Smith, D. Graham, *Appl. Spectrosc.* **2008**, 62, 371-376.

57. F. Inscore, C. Shende, A. Sengupta, H. Huang, S.Farquharson, *Appl. Spectrosc.* **2011**, 65, 1004-1008.

58. R. M. Jarvis, R. Goodacre, *Chem. Soc. Rev.* **2008**, 37, 931-936.

59. B. H. Liu, G. M. Han, Z. P. Zhang, R. Y. Liu, C. L. Jiang, S. H. Wang, M. Y. Han, *Anal. Chem.* **2012,** 84, 255-261.

60. X. H. Jiang, Y. C. Lai, M. Yang, H. Yang, W. Jiang, J. H. Zhan, *Analyst* **2012**, 137, 3995-4000.

61. M. L. Cheng, Y. Yang, *J. Raman Spectrosc.* **2010**, 41, 167-174.

62. C. Battocchio, C. Meneghini, L. Fratoddi, I. Venditti, M. V. Russo, G. Aquilanti, C. Maurizio, F. Bondino, R. Matassa, M. Rossi, S. Mobilio, G. Polzonetti, *J. Phys. Chem. C.* **2012**, 116, 19571-19578.

63. Y. C. Lai, J. C. Cui, X. H. Jiang, S. Zhu, J. H. Zhan, *Analyst* **2013**, 138, 2598-2603.

64. A. Kudelski, *J. Raman Spectrosc.* **2003**, 34, 853-862.

65. N. D. Strekal, A. E. German, G. A. Gachko, S. A. Maskevich, *Optics and Spectroscopy* **2000**, 89, 834–840.

66. C. L. Jones, K. C. Bantz, C. L. Haynes, *Anal. Bioanal. Chem.* **2009**, 394, 303-311.

67. B. J. Kennedy, S. Spaeth, M. Dickey, K. T. Carron, *J. Phys. Chem. B.* **1999**, 103, 3640-3646.

68. J. M. McMahon, A. I. Henry, K. L. Wustholz, M. J. Natan, R. G. Freeman, R. P. Van Duyne, G. C. Schatz, *Anal. Bioanal. Chem.* **2009**, 394, 1819-1825.

69. A. Otto, H. Grabhorn, W. Akemann, *J. Phys.: Condens. Matter* **1992**, *4*, 1143-1212.

70. L.-L. Qu, D.-W. Li, J.-Q. Xue, W.-L. Zhai, J. S. Fossey, Y.-T. Long, *Lab Chip* **2012**, 12, 876-881.

71. D. He, B. Hu, Q.-F. Yao, K. Wang, S.-H. Yu, *ACS Nano* **2009**, 12, 3993-4002.

72. K. Kneipp, H. Kneipp, I. Itzkan, R. R. Dasari, M. S. Feld, *Chem. Rev.* **1999**, 99, 2957-2975.

73. R. W. Walters, R. G. Luthy, *Environ. Sci. Technol.* **1984,** 16, 395-403.

74. M. A. Bryant, J. E. Pemberton, *J. Am. Chem. Soc.* **1991**, 113, 3629-3637.

Analyst Accepted Manuscript